Journal of Power Sources 183 (2008) 84–91

Contents lists available at ScienceDirect

Journal of Power Sources

journal homepage: www.elsevier.com/locate/jpowsour

Electro-deposition on carbon black and carbon nanotubes of Pt nanostructured catalysts for methanol oxidation

Claudia Paoletti[a,*], Alessia Cemmi[a], Leonardo Giorgi[b], Rossella Giorgi[b], Luciano Pilloni[b], Emanuele Serra[b], Mauro Pasquali[c]

[a] ENEA R.C. Casaccia, TER, Via Anguillarese 301, IT-00123 Rome, Italy
[b] ENEA R.C. Casaccia, FIMMATTEC, Via Anguillarese 301, IT-00123 Rome, Italy
[c] Department of Materials Engineering, La Sapienza University, Via del Castro Laurenziano 7, IT-00161 Rome, Italy

ARTICLE INFO

Article history:
Received 4 March 2008
Received in revised form 14 April 2008
Accepted 20 April 2008
Available online 8 May 2008

Keywords:
PEFCs
Electro-deposition techniques
Pt electro-catalysts
Electro-catalytic activity

ABSTRACT

An electrochemical method for the Pt nanoparticles deposition on porous and high surface carbon substrates (carbon black and carbon nanotubes), as an alternative way to prepare gas diffusion electrodes for polymer electrolyte fuel cells (PEFCs), is herein described. Pt nanoparticles well distributed and localized on the electrode surface were obtained by using an electric field. The electro-catalysts were prepared by single and multiple pulse galvanostatic polarizations in 1 M sulphuric acid + 5 mM exachloroplatinic acid solution. Chemical analysis, cyclic voltammetry and field emission gun scanning electron microscopy were used to determine the electrochemical features of Pt deposits and the influence of electro-deposition method on their nano-morphology. Electro-catalytic performances were studied by investigating the methanol oxidation reaction and the results are presented in form of surface specific activity and mass specific activity to take into account the electrochemical real surface and Pt loading. A comparison with commercial E-TEK Pt/C catalysts, prepared by traditional chemical reduction and heat treatment in hydrogen, shows that the electrodeposited catalyst presents higher activity at lower Pt loading.

© 2008 Elsevier B.V. All rights reserved.

1. Introduction

Polymer electrolyte fuel cells (PEFCs) and direct methanol fuel cells (DMFCs) have high potentiality for use in electric power production, for consumer electronics and portable power applications, due to their good energy conversion efficiency and high power density [1]. However, their commercial diffusion still needs further electrode materials and catalysts improvement to enhance their performances.

DMFC has a significant advantage for powering portable applications since it does not require a separate hydrogen generation system. Methanol is attractive as a fuel because it is cheap, widely available, and can be handled and distributed easily. However, electro-oxidation of methanol is a very complex reaction involving many poisonous intermediate species [2–5]. In acidic medium, Pt shows high performances towards methanol oxidation reaction. The electro-catalytic activity of Pt particles depends on many factors, such as particle size and dispersion [6–10], preparation methods [11,12], supporting materials [5,13,14,15]. Generally, small Pt particles homogeneously dispersed result in a high electro-catalytic activity [16]. Simultaneously, decrease of noble metal loading is also necessary for cost abatement [17,18].

Pt electro-catalysts are traditionally prepared by carbon support impregnation with a Pt precursor, followed by chemical reduction and heat treatment in hydrogen [19–23]. This method requires a high amount of Pt (>0.3 mg cm^{-2}) to achieve good performances because nanoparticles localization in reaction sites results critical. Moreover, most of traditional techniques usually involve tedious and time-consuming treatments wherein impurities can be easily taken up from the bath solution, which may cause catalyst deterioration.

Electrochemical techniques are gaining more and more interest due to their advantages, such as a simple procedure for deposition, high purity of deposits and easy control of the loading mass [24,25]. Recent studies show that the use of an electric field in the catalyst deposition directs the localization of Pt nanoparticles only in the active reaction sites accessible both to electrons and protons (carbon substrate/electro-catalyst/membrane triple interface), leading to a high lowering of Pt loading (<0.1 mg cm^{-2}) [26–29].

Also, supporting materials have been demonstrated to play a key role in determining the activity of supported catalyst [30,31].

* Corresponding author. Tel.: +39 0630483169; fax: +39 0630486357.
E-mail address: claudia.paoletti@casaccia.enea.it (C. Paoletti).

0378-7753/$ – see front matter © 2008 Elsevier B.V. All rights reserved.
doi:10.1016/j.jpowsour.2008.04.083

Namely, a high surface carbon support is required to couple a high catalytic activity to a low Pt-loading. Up to now, one of the most-used support for Pt electro-catalysts is Vulcan XC-72R carbon black. Despite its high surface area enhances catalyst dispersion, the presence of a micro-porous structure (<2 nm diameter) can induce a poor Pt utilization, as Pt particles localized in the micro-pores are inaccessible to methanol molecules. Furthermore, carbon blacks could contain sulphur groups and may cause aggregation of Pt particles [32]. Beside carbon blacks, carbon nanotubes are receiving increasing attention as catalyst supports [33–38] because of their uncommon properties, nanometric size and high surface area. Some authors [39–41] have shown that carbon nanotubes induce a higher catalytic activity towards methanol oxidation than conventional Vulcan XC-72R, even though the reason is still unclear.

In this work, Pt nanoparticles electro-catalysts were deposited on different carbon substrates (carbon black and carbon nanotubes) by means of galvanostatic polarization techniques. These are usually preferred to potentiostatic techniques [42], because they allow for a better control of parameters and an easier industrial scale-up. The nanoscale morphology of the electrodes was examined with scanning electron microscopy. The electrochemical real surface was determined by cyclic voltammetry in sulphuric acid solution while the electro-catalytic activity was estimated from the charge involved in the methanol oxidation reaction.

2. Experimental

Carbon black Vulcan XC72R Cabot Co. (CB, BET surface area 191 $m^2\,g^{-1}$) and Multiwall Carbon Nanotubes supplied by Chinese Academy of Science (CNTs, BET surface area 50 $m^2\,g^{-1}$) were used as carbon substrates. In order to remove graphitic nanoparticles, amorphous carbon and catalyst impurities, CNTs were pre-treated in boiling 2 M HNO_3 aqueous solution for 1 h.

A standard three-electrodes cell was employed. A high purity (99.9999%) Pt foil served as counter electrode, an Ag/AgCl saturated electrode (SSC) was used as reference electrode and the working electrode was prepared as reported below.

A homogeneous alcoholic suspension of CB or CNTs mixed with Nafion® solution (DuPont) was sprayed over a cleaned glassy carbon disc, inserted in a Teflon holder, with a geometric surface of 0.125 cm^2 and then dried. This device, as prepared, is ready to the Pt deposition.

Pt nanoparticles were electrodeposited on the substrates by galvanostatic polarization from 5 mM H_2PtCl_6 + 1 M H_2SO_4 aqueous solution. Deposition parameters for the galvanostatic electro-deposition at constant (GED) and pulsed current (PED) were afterwards defined. In Fig. 1a inset, a typical GED pulse profile is shown: t_p is the polarization time and i_p is the applied current density. Electro-deposition charge density (Q_{ED}) is calculated as the product between i_p and t_p. In this work, the following parameters t_p = 300 s and i_p varying from 0.025 to 0.3 mA cm^{-2} were used.

PED current profile is reported in Fig. 1b inset, characterized by three parameters: the current on time t_{on}, the current off time t_{off} and the applied current density i_p.

The average applied current density $i_{m,ED}$ and the average electro-deposition charge density $Q_{m,ED}$ can be calculated by these equations [43], where t_{ptot} is the total polarization time:

$$i_{m,ED} = i_p \left(\frac{t_{on}}{t_{on} + t_{off}} \right) \quad (1)$$

$$Q_{m,ED} = i_p \left(\frac{t_{on}}{t_{on} + t_{off}} \right) t_{ptot} \quad (2)$$

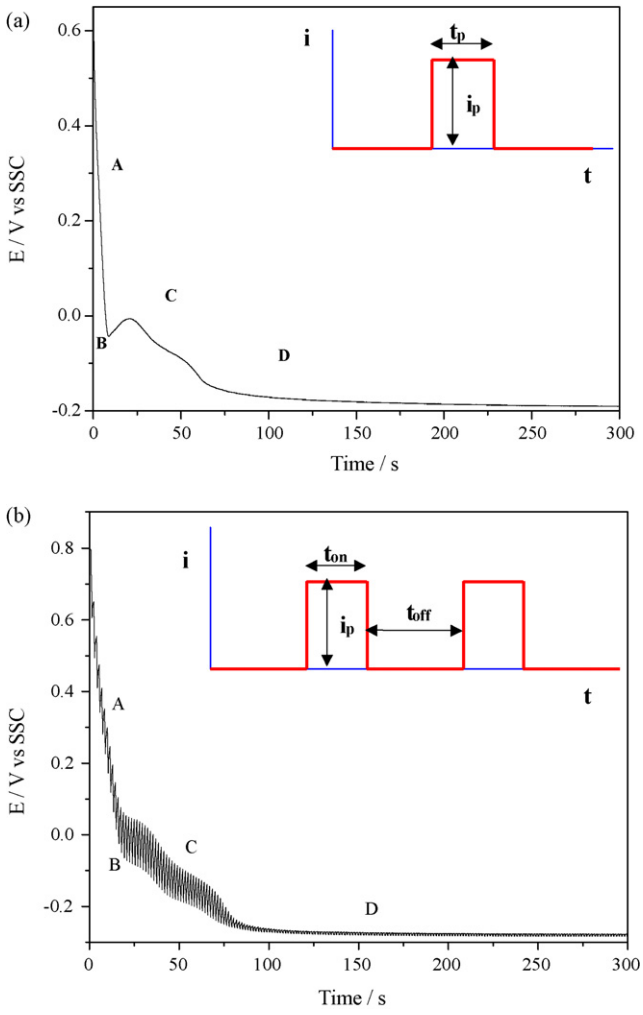

Fig. 1. Chronopotentiometric curve in H_2SO_4 1 M + H_2PtCl_6 5 mM of Pt deposited on carbon substrates by galvanostatic polarization at (a) single and (b) multiple pulses. A–D represent the main steps of nucleation process. Inset: (a) typical single pulse galvanostatic electro-deposition (GED) where t_p is the polarization time and i_p is the applied current density; (b) typical multiple pulses galvanostatic electro-deposition (PED) where t_{on} is the current on time, t_{off} is the current off time and i_p is the applied current density.

For PED depositions, constant t_{ptot} = 300 s, t_{on} = 0.5 s and t_{off} = 1.0 s were applied.

Applied current density was systematically investigated between 0.075 and 0.9 mA cm^{-2}.

Electrochemical properties and electro-catalytic activity of Pt/CNTs and Pt/CB deposits were investigated by cyclic voltammetry (CV) in 1 M H_2SO_4 and 1 M H_2SO_4 + 0.5 M CH_3OH aqueous solution, respectively. CVs were recorded at scan rate of 100 mV s^{-1} with potential cycled between −0.2 and +1.3 V vs. SSC. Electro-deposition tests, electrochemical and electro-catalytic characterizations were carried out using a potentiostat–galvanostat PAR EG&G mod. 273A. Before all these measurements, the solution was purged with N_2 for 30 min to eliminate O_2. During the experiments, N_2 was only introduced into the cell above the solution and used as the protecting atmosphere. All experiments were carried out at room temperature.

Highly dispersed Pt/CB and Pt/CNTs catalysts morphology and particle size distribution were studied by field emission gun scanning electron microscopy, FEG-SEM (LEO mod. 1530).

3. Results and discussion

3.1. Electro-deposition and electrochemical characterization of Pt particles on carbon substrates

The electro-crystallization process, consisting in a solid phase formation by reduction of a metal ion solution [44], has been extensively studied and several thermodynamic and kinetic models have been proposed [45–51].

Chronopotentiometric responses of GED (Fig. 1a) and PED (Fig. 1b) present four different steps due to electro-crystallization process:

- A: Pt chlorine-complex adsorption to electrode surface and ad-ions generation;
- B: ad-ions change to ad-atoms due to charge transfer and formation of a high nuclei number;
- C: growth of the deposited nuclei to obtain Pt clusters;
- D: Pt macro-cluster generation developing towards a full covering of the electrode surface.

As observed, the ion diffusion toward the electrode surface and the following electron transfer (A and B) are nearly fast, while the rate determining steps correspond to the ad-atoms surface diffusion to form Pt clusters (C and D), probably due to the partially solvation of metal ions.

By means of CV the electrochemical behavior of Pt deposits is investigated: at low potential, between −0.3 and +0.2 V, typical peaks related to hydrogen adsorption/desorption are evident as well as the peaks due to Pt oxide monolayer formation and reduction at higher potential (Fig. 2).

The electrochemical real surface (ERS) was calculated by the charge density required for hydrogen desorption (Q_{Hdes}) from Pt surface, after subtraction of the electrochemical double layer current density. The ERS value of Pt deposits was calculated from Q_{Hdes} (mC) by using the factor Q_{ref} = 0.21 mC related to an atomically 1 cm^2 smooth Pt electrode [52].

$$\mathrm{ERS} = \frac{Q_{\mathrm{Hdes}}}{Q_{\mathrm{ref}}} \quad (3)$$

GED and PED Pt deposits ERS was reported vs. electro-deposition charge density (Q_{ED}) in Fig. 3a and b. A significant ERS increase before 200 mC cm^{-2} is probably related to a sudden surface coverage by Pt nanoparticles. At higher Q_{ED}, GED trend presents a maximum at 360 mC cm^{-2} while PED is characterized by a plateau. Comparing these plots, GED deposition achieves ERS value generally higher than PED (20–40 cm^2 vs. 15–25 cm^2). Note that CNTs substrate enhances even more ERS.

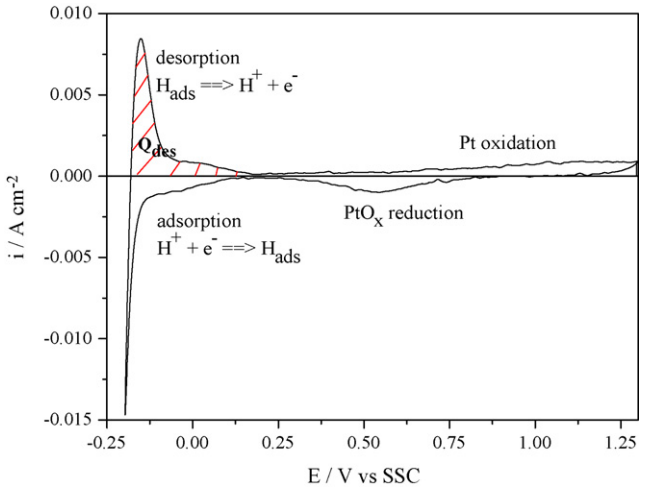

Fig. 2. Cyclic voltammetry of Pt deposited on carbon substrates in 1 M H_2SO_4 at 100 mV s^{-1}.

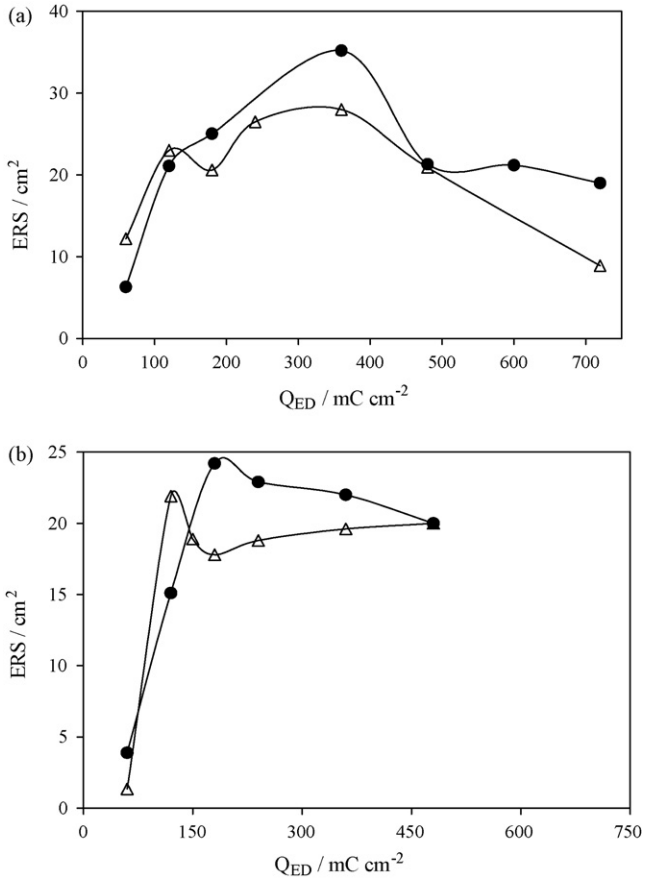

Fig. 3. Electrochemical real surface vs. electro-deposition charge density trend of GED and PED Pt electro-catalysts: (a) GED (-Δ-) Pt/CB, (-●-) Pt/CNTs and (b) PED (-Δ-) Pt/CB, (-●-) Pt/CNTs.

3.2. Influence of morphology on the electro-catalytic performances

FEG-SEM micrographs at 30,000× in Figs. 4 and 5 are reported, for GED and PED deposits respectively: as observed, Pt nanoparticles are well dispersed on CB and on CNTs surfaces.

In particular, for GED deposits (Fig. 4) it is clear that at the lowest charge density (i.e. 180 mC cm^{-2}) the size of Pt particles is homogeneous, while at the highest value (i.e. 240 mC cm^{-2}) the presence of small Pt particles is detected, indicating a new nucleation process.

PED deposits (Fig. 5) present differently sized Pt particles at 180 mC cm^{-2} and a more uniform distribution at 360 mC cm^{-2}.

Comparing Figs. 4a and 5a, despite the same charge density value, CB substrate shows two completely different behaviors in GED and PED. The former gives a lower Pt surface coverage than the latter but a more uniform particle size distribution.

SEM images at 150,000× are reported in Figs. 6–9. It is possible to distinguish three different morphologies: spherical (Figs. 6a, b, 7a, 8a, 9a), dendritic (Figs. 7b, 9b, c) and lamellar shape (Figs. 6d, 7c, d, 8b, c, d, 9d).

Pt deposited by GED on CB (Fig. 6) presents almost the same spherical morphology up to 360 mC cm^{-2}, while the preferential

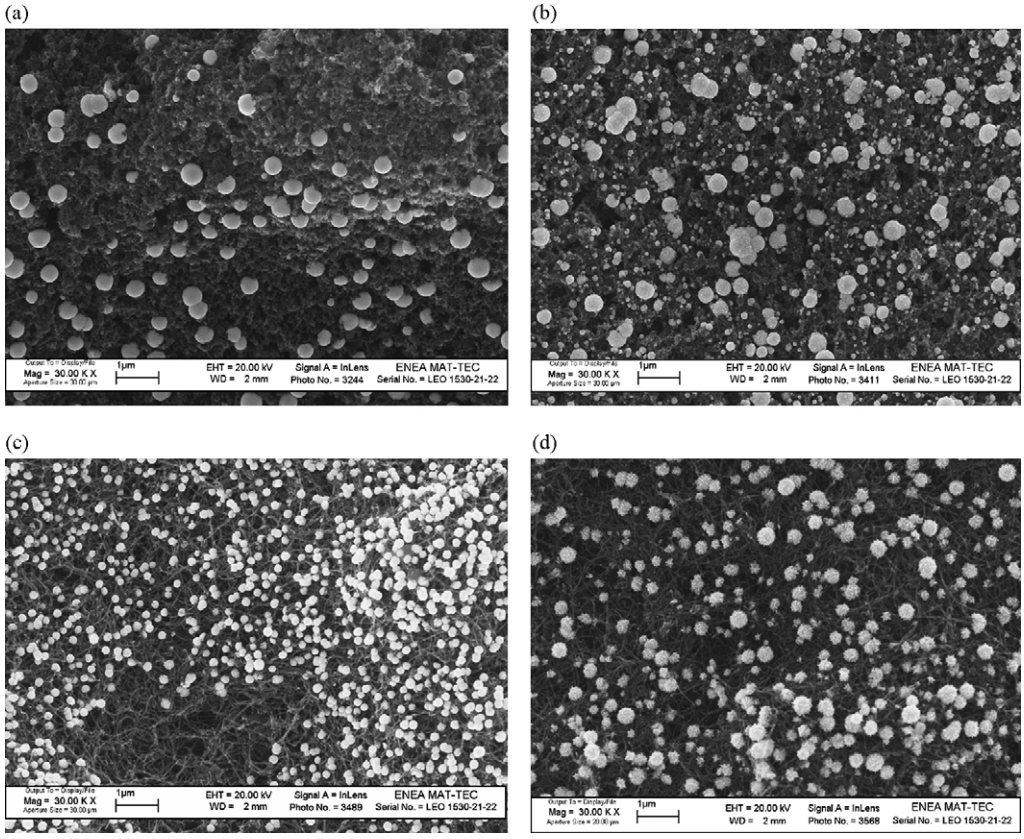

Fig. 4. SEM images at 30,000× magnification of deposits prepared by GED: (a) Pt/CB at 180 mC cm^{-2}; (b) Pt/CB at 240 mC cm^{-2}; (c) Pt/CNTs at 180 mC cm^{-2} and (d) Pt/CNTs at 240 mC cm^{-2}.

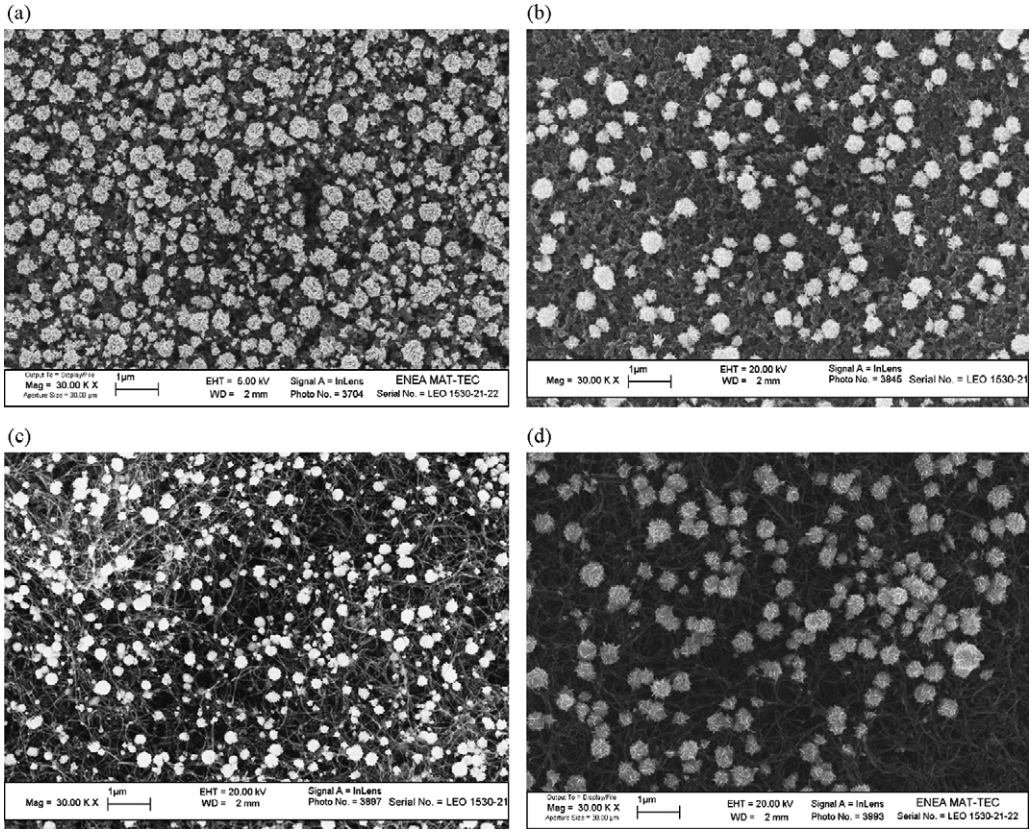

Fig. 5. SEM images at 30,000× magnification of deposits prepared by PED: (a) Pt/CB at 180 mC cm^{-2}; (b) Pt/CB at 360 mC cm^{-2}; (c) Pt/CNTs at 180 mC cm^{-2} and (d) Pt/CNTs at 360 mC cm^{-2}.

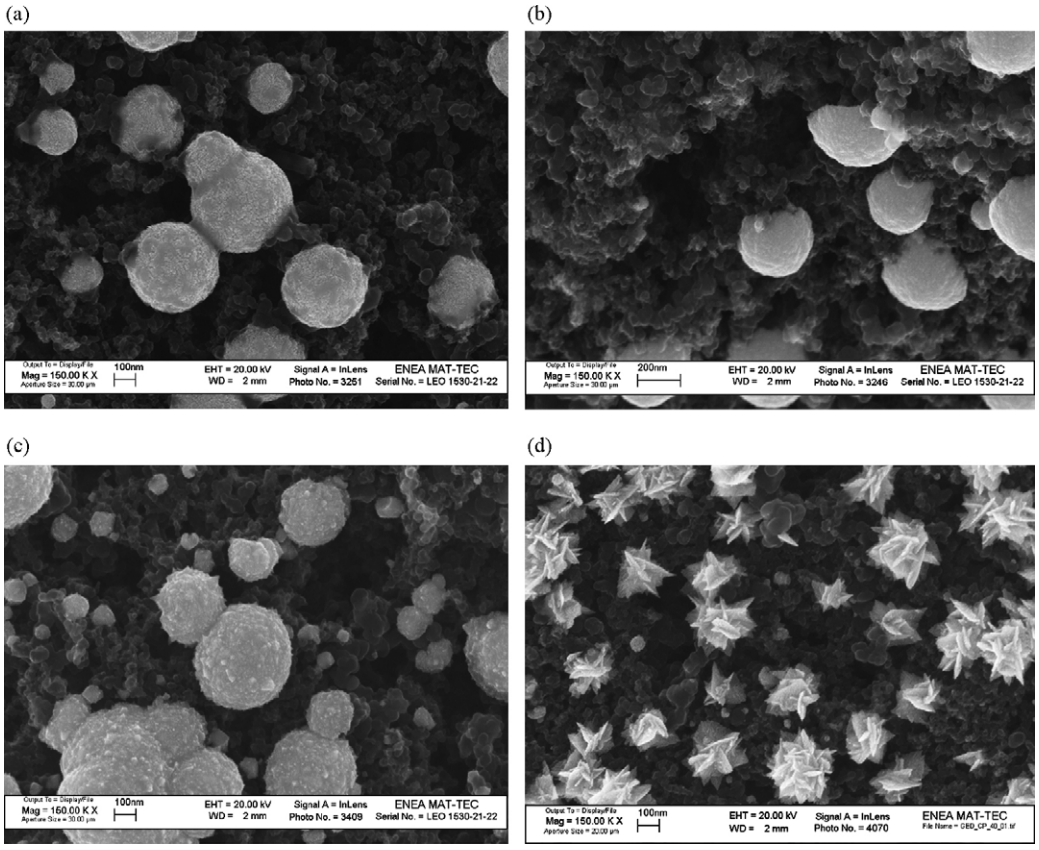

Fig. 6. SEM images at 150,000× magnification of deposits prepared by GED on CB at: (a) 120 mC cm^{-2}; (b) 180 mC cm^{-2}; (c) 240 mC cm^{-2} and (d) 360 mC cm^{-2}.

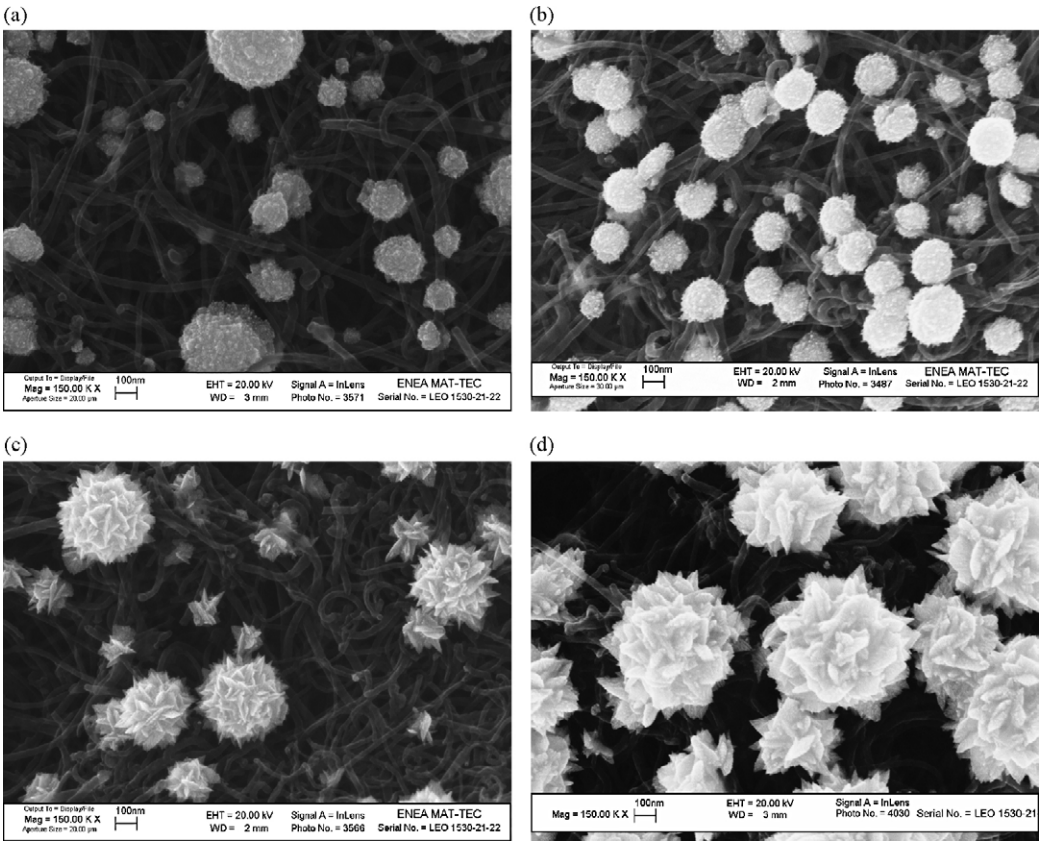

Fig. 7. SEM images at 150,000× magnification of deposits prepared by GED on CNTs at: (a) 120 mC cm^{-2}; (b) 180 mC cm^{-2}; (c) 240 mC cm^{-2} and (d) 360 mC cm^{-2}.

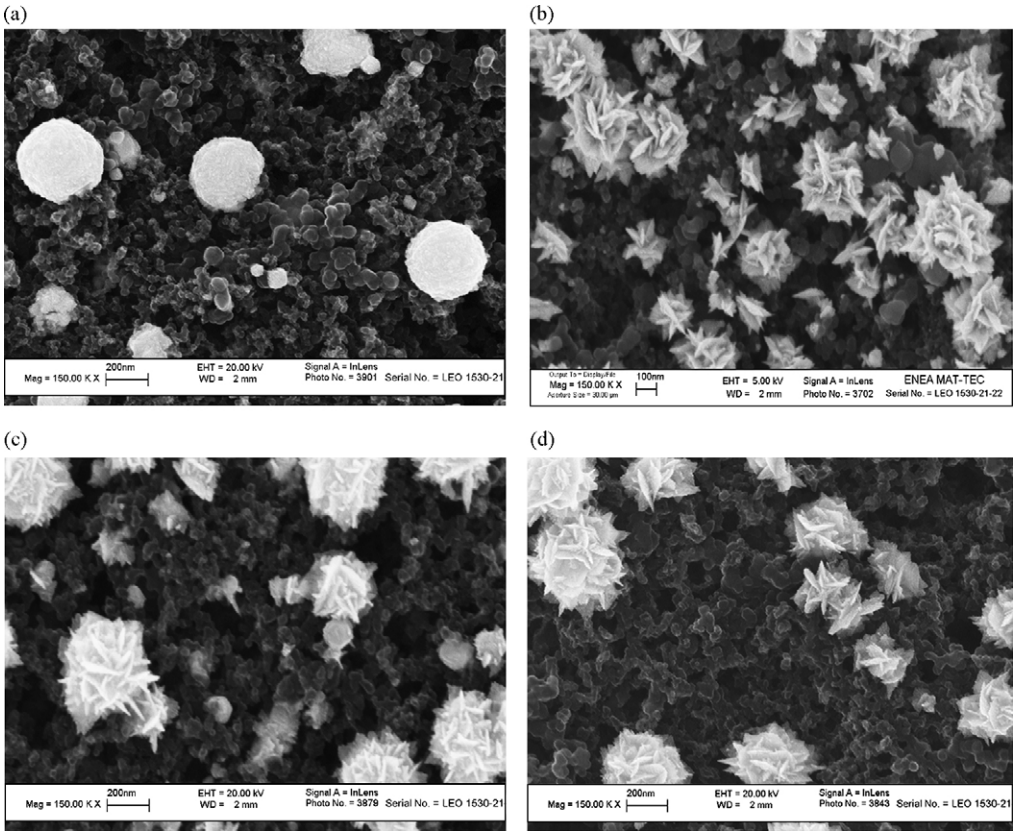

Fig. 8. SEM images at 150,000× magnification of deposits prepared by PED on CB at: (a) 120 mC cm^{-2}; (b) 180 mC cm^{-2}; (c) 240 mC cm^{-2} and (d) 360 mC cm^{-2}.

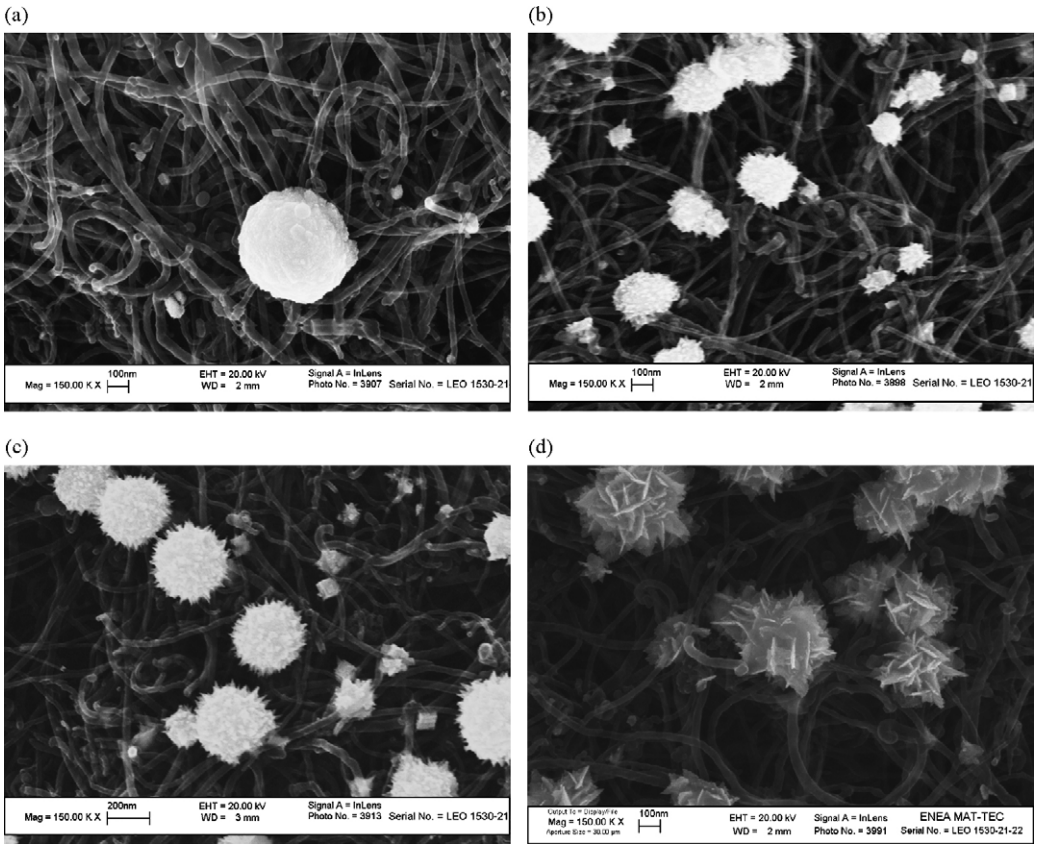

Fig. 9. SEM images at 150,000× magnification of deposits prepared by PED on CNTs at: (a) 120 mC cm^{-2}; (b) 180 mC cm^{-2}; (c) 240 mC cm^{-2} and (d) 360 mC cm^{-2}.

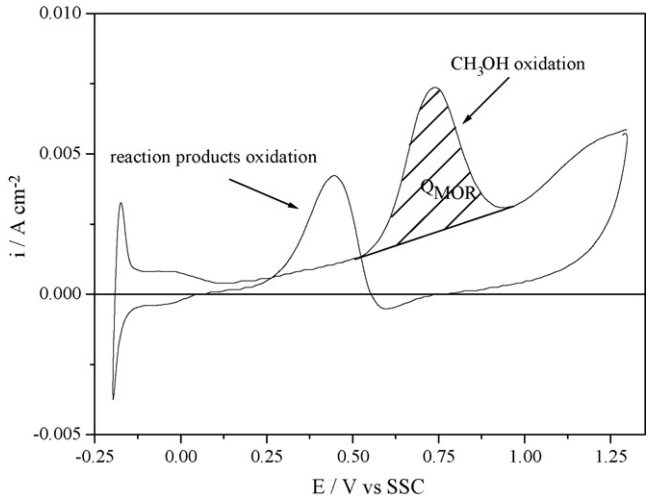

Fig. 10. Cyclic voltammetry of Pt deposited on carbon substrates in 1 M H_2SO_4 + 0.5 M CH_3OH at 100 mV s^{-1}.

growth obtained by PED is a lamellar structure starting already from 180 mC cm^{-2} (Fig. 8).

CNTs deposits obtained by both the electro-deposition techniques display very similar morphologies accordingly with the charge density values. Hence, spherical at 120 mC cm^{-2}, dendritic between 180–240 mC cm^{-2} and lamellar at 360 mC cm^{-2} (Figs. 7 and 9).

It is worth noticing that for all the electro-catalysts, both lamellar and spherical shapes present an extremely fine nanostructured Pt surface (2–4 nm), as clearly evidenced by their SEM micrographs at 1,000,000× (not shown here).

In Fig. 10 CV recorded in 1 M H_2SO_4 + 0.5 M CH_3OH is reported. Two peaks, beside the hydrogen adsorption/desorption peaks previously described, are evident: the one (0.5–0.9 V) referred to the methanol oxidation while the other (0.25–0.6 V) to the oxidation of previously formed by-products (e.g. CO, HCOOH, HCHO, etc.).

The methanol oxidation reaction (MOR) activity was determined by the charge density required for the methanol oxidation (Q_{MOR}). The catalytic activity was evaluated as surface specific activity (SSA) and mass specific activity (MSA) according to the following equations:

$$SSA = \frac{Q_{MOR} S_g}{ERS} \quad (4)$$

$$MSA = \frac{Q_{MOR}}{L_{Pt}} \quad (5)$$

where S_g is the working electrode geometric surface and L_{Pt} is the Pt loading (Table 1), calculated by SEM elaborated images with JmageJ 1.33a software [53].

In Fig. 11 electro-catalysts SSA trends are reported and compared with E-TEK 10 wt% Pt/C commercial catalyst.

The best results are shown by Pt electro-catalysts deposited by GED on CNTs (GED-CNTs) and by PED on CB (PED-CB). Moreover, all deposits, except Pt electro-catalysts deposited by GED on CB,

Table 1
Pt loading (L_{Pt}) of GED and PED deposits and of E-TEK commercial catalyst

Sample	L_{Pt} (mg cm^{-2})
GED Pt/CB	0.113
GED Pt/CNTs	0.068
PED Pt/CB	0.097
PED Pt/CNTs	0.055
E-TEK	0.300

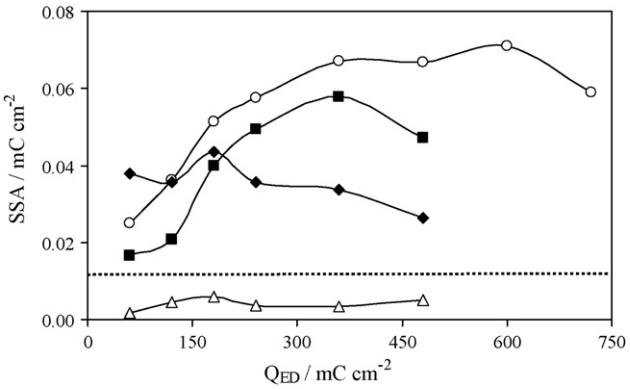

Fig. 11. Specific surface activity vs. electro-deposition charge density of GED and PED Pt electro-catalysts: (-Δ-) GED Pt/CB; (-■-) PED Pt/CB; (-○-) GED Pt/CNTs; (-♦-) PED Pt/CNTs and commercial E-TEK 10 wt% Pt/C electro-catalyst (dotted line).

present a higher SSA than that of commercial E-TEK catalyst, even if the latter has the highest ERS (about 100 cm^2).

Comparing MOR results and morphological analysis, it is possible to find a significant correlation between electro-catalytic behaviors and nanoparticles structure.

A lamellar growth corresponds to higher SSA values of GED-CNTs and of PED-CB deposits.

Generally, upon increasing Q_{ED} a greater Pt deposition on carbon substrate is expected, but SSA values from electro-catalysts obtained by GED and PED actually do not rise when a Q_{ED} > 300 mC cm^{-2} is applied. A possible explanation can be proposed considering edges and tips formation on the uppermost surface of Pt nanoparticles: in fact, just next to these structures, a high methanol concentration gradient is produced. Only the Pt here localized, directly in contact with methanol, can give rise to the catalytic reaction.

Performances of GED and PED deposits result even more significant with respect to those of the commercial catalyst, if a comparison is made between their corresponding mass specific activity (MSA) values, which take into account the Pt loading.

In Fig. 12 E-TEK catalyst and the best electro-deposited GED-CNTs are compared. The latter presents a considerable activity improvement towards MOR, even though the Pt loading (L_{Pt} < 0.1 mg cm^{-2}) is three times lower than that of E-TEK (L_{Pt} > 0.3 mg cm^{-2}). These results suggest that in E-TEK catalyst a

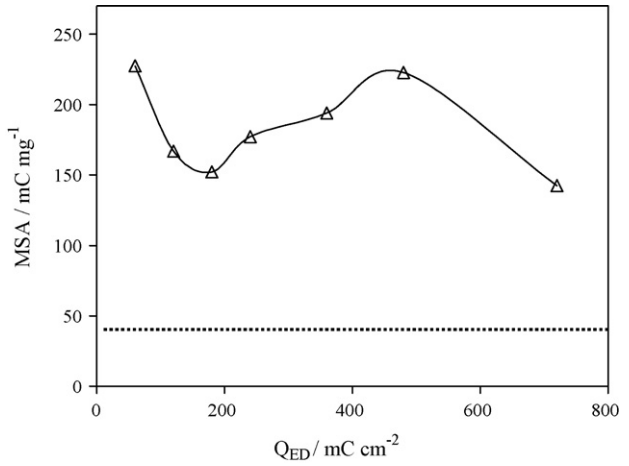

Fig. 12. Mass specific activity vs. electro-deposition charge density comparison between GED Pt/CNTs electro-catalyst (-Δ-) and commercial E-TEK 10 wt% Pt/C electro-catalyst (dotted line).

large amount of Pt, probably positioned too deeply in the carbon bulk, is inactive in MOR because methanol molecules cannot reach the catalytic sites. Conversely, these evidences confirm that the electro-deposition technique allows to deposit Pt particles effectively on the uppermost part of the carbon substrates, diminishing the catalyst loading and the DMFCs whole cost.

4. Conclusions

By means of galvanostatic polarization with single and multiple pulse, highly dispersed Pt nanoparticles on carbon black and on multiwall carbon nanotubes were electro-deposited.

Pt deposits with a fine nanostructured surface as well as uniform electro-catalyst distribution on both CB and CNTs substrates were obtained. Electro-deposition parameters allow to significantly control the Pt particles morphology, leading to spherical, dendritic and lamellar shapes.

The use of an electric field to deposit catalyst particles presents many advantages with respect to the traditional preparation methods, among which the absence of reducing as well as deflocculating agents and of heat treatments in hydrogen.

Pt electro-catalysts obtained from GED show electrochemical real surface values generally higher than those of PED deposits. Moreover, both electro-deposition techniques give a limited ERS growth upon increasing Q_{ED}, because the Pt amount in excess is not localized in the triple reaction interface, but contributes to the dendritic and lamellar formation.

Electro-catalytic properties show that methanol oxidation reaction is influenced by the deposit morphology: nanostructured globular surface shapes give the best electro-catalytic performances. Pt/CB obtained by PED achieves the same activity of Pt/CNTs by GED, but the latter has a lower Pt loading.

Finally, the best electro-catalyst prepared in this work (Pt/CNTs by GED) shows a MOR activity higher than that of E-TEK commercial catalyst with a three times higher Pt loading.

Acknowledgements

Multiwall carbon nanotubes have been supplied by Dr. Gang Wang and produced in Beijing National Laboratories for Condensed Matter, Institute of Physics, Chinese Academy of Science (PRC).

References

[1] A.J. Appleby, F.R. Foulkes, Fuel Cell Handbook, Van Norstand Reinhold, New York, NY, 1989.
[2] Z. He, J. Chen, D. Liu, H. Tang, W. Deng, Y. Kuang, Mater. Chem. Phys. 85 (2004) 396–401.
[3] J.-M. Leger, J. Appl. Electrochem. 31 (2001) 767.
[4] H. Wang, T. Loffler, H. Baltruschat, J. Appl. Electrochem. 31 (2001) 759.
[5] F. Gloaguen, J.-M. Leger, C. Lamy, J. Appl. Electrochem. 27 (1997) 1052.
[6] S. Katsuaki, U. Kohei, K. Hideaki, N. Yoshinobu, J. Electroanal. Chem. 256 (1988) 481.
[7] M. Watanabe, S. Saegusa, P. Stonehart, J. Electroanal. Chem. 271 (1989) 213.
[8] S. Katsuaki, I. Ryuhei, K. Hideaki, J. Electroanal. Chem. 284 (1990) 523.
[9] N. Giordano, E. Passalacqua, L. Pino, A. Arico', V. Antonucci, M. Vivaldi, K. Kinoshita, Electrochim. Acta 36 (1991) 1979.
[10] J.H. Ye, P.S. Fedkiw, Electrochim. Acta 41 (1996) 221.
[11] Z. Liu, L.M. Gan, L. Hong, W. Chen, J.Y. Lee, J. Power Sources 139 (2005) 73.
[12] M.J. Escudero, E. Hontanon, S. Schwartz, M. Boutonnet, L. Daza, J. Power Sources 106 (2002) 206.
[13] H. Tang, J. Chen, S. Yao, L. Nie, Y. Kuang, Z. Huang, D. Wang, Z. Ren, Mater. Chem. Phys. 92 (2005) 548.
[14] Z.D. Wei, S.H. Chan, L.L. Li, H.F. Cai, Z.T. Xia, C.X. Sun, Electrochim. Acta 50 (2005) 2279.
[15] L. Giorgi, T.D. Makris, R. Giorgi, N. Lisi, E. Salernitano, Sens. Actuators B 126 (2007) 144.
[16] Y. Takasu, W. Sugimoto, Y. Muratami, Catal. Surv. Asia 7 (1) (2003) 21.
[17] E. Passalacqua, F. Lufrano, G. Squadrito, A. Patti, L. Giorgi, Electrochim. Acta 43 (24) (1998) 3665.
[18] D.N. Prader, J.J. Rusek, Appl. Energy 74 (2003) 135.
[19] H.E. Van Dam, H. Van Bekkum, J. Catal. 131 (1991) 335.
[20] M. Watanabe, M. Uchida, S. Motoo, J. Electroanal. Chem. 229 (1987) 395.
[21] H.G. Petrow, R.J. Allen, U.S. Patent no. 4,044,193 (1977).
[22] H. Huang, W. Zhang, M. Li, Y. Gan, J. Chen, Y. Kuang, J. Colloid Interface Sci. 284 (2005) 593.
[23] N. Rajalakshmi, H. Ryu, M.M. Shaijumon, S. Ramaprabhu, J. Power Sources 140 (2005) 250.
[24] H. Kim, N.P. Subramanian, B.N. Popov, J. Power Sources 138 (2004) 14.
[25] H. Natter, R. Hempelmann, Electrochim. Acta 49 (2003) 51.
[26] L. Giorgi, A. Pozio, E. Antolini, J. Power Sources 77 (1999) 136.
[27] K.H. Choi, H.S. Kim, T.H. Lee, J. Power Sources 75 (1998) 230.
[28] H. Kim, B.N. Popov, Electrochem. Solid-State Lett. 7 (4) (2004) A71.
[29] F. Lufrano, E. Passalacqua, G. Squadrito, A. Patti, L. Giorgi, J. Appl. Electrochem. 29 (1999) 445.
[30] J.-S. Yu, S. Kang, S.B. Yoon, G. Chai, J. Am. Chem. Soc. 124 (2002) 9382.
[31] J.A. Bennet, Y. Show, S. Wang, G.M. Swain, J. Electrochem. Soc. 152 (2005).
[32] S.C. Roy, et al., J. Electrochem. Soc. 143 (1996) 3073.
[33] V. Lordi, N. Yao, J. Wei, Chem. Mater. 13 (2001) 733.
[34] G.L. Che, B.B. Lakshmi, C.R. Martin, E.R. Fisher, Langmuir 15 (5) (1999) E184.
[35] Z.L. Liu, X.H. Lin, J.Y. Lee, W. Zhang, M. Han, L.M. Gan, Langmuir 18 (10) (2002) 4054.
[36] W. Li, C. Liang, J. Qiu, W. Zhou, H. Han, Z. Wie, G. Sun, et al., Carbon 40 (2002) 791.
[37] B. Rajesh, V. Karthik, S. Karthikeyan, K.R. Thampi, J.M. Bonard, B. Viswanathan, Fuel 80 (17) (2002) 2177.
[38] C. Wang, M. Waie, X. Wang, J.M. Tang, R.C. Haddon, Y. Yan, Nano Lett. 4 (2) (2004) 345.
[39] G. Wu, Y.-S. Chen, B.-Q. Xu, Electrochem. Commun. 7 (2005) 1237.
[40] T. Matsumoto, T. Komatsu, H. Nakano, K. Arai, Y. Nagashima, E. Yoo, T. Yamazaki, M. Kijima, H. Shimizu, Y. Takasawa, J. Nakamura, Catal. Today 90 (2004) 277.
[41] H.J. Wang, H. Yu, F. Peng, P. Lv, Electrochem. Commun. 8 (2006) 499.
[42] S. Liu, Z. Tang, E. Wang, S. Dong, Electrochem. Commun. 2 (2000) 800.
[43] J.C. Puippe, F. Leamen, Theory Practice of Pulse Plating, America Electroplaters and Surface Finishers Society, Orlando, 1986.
[44] R. Greef, R. Peat, L.M. Peter, D. Pletcher, J. Robinson, Instrumental Methods in Electrochemistry, Ellis Horwood Limited, Chichester, UK, 1985.
[45] M. Peykova, E. Michailova, D. Stoychev, A. Milchev, Electrochim. Acta 40 (1995) 2601.
[46] O. Antoine, R. Durand, Electrochem. Solid State Lett. 4 (2001) A55.
[47] M.S. Lofler, B. Gross, H. Natter, R. Hempelmann, Th. Krajewski, J. Divisek, Phys. Chem. Chem. Phys. 3 (2001) 333.
[48] E. Zinigrad, D. Aurbach, P. Dan, Electrochim. Acta 46 (2001) 1863.
[49] A. Milchev, E. Michailova, R. Lacmann, B. Muller-Zulow, Electrochim. Acta 38 (1993) 535.
[50] A. Milchev, R. Lacmann, Electrochim. Acta 40 (1995) 1475.
[51] E. Michailova, A. Milchev, R. Lacmann, Electrochim. Acta 41 (1996) 329.
[52] A.J. Bard, Electroanalytical Chemistry, vol. 9, Marcel Dekker, 1976.
[53] W. Rasband, National Institute of Health, USA, http://rsb.info.nih.gov/ij/.